EARTH SURFACE PROCESSES AND LANDFORMS
Earth Surf. Process. Landforms (2017)

Published online in Wiley Online Library
(wileyonlinelibrary.com) DOI: 10.1002/esp.4167

Late Holocene mangrove dynamics dominated by autogenic processes

Caio A. Moraes,[1] Neuza A. Fontes,[1] Marcelo C.L. Cohen,[1]* Marlon Carlos França,[2] Luiz C.R. Pessenda,[3] Dilce F. Rossetti,[4] Mariah I. Francisquini,[3] José A. Bendassolli[5] and Kita Macario[6]

[1] Graduate Program of Geology and Geochemistry, Federal University of Pará, Belém, Brazil
[2] Federal Institute of Pará, Belém, Brazil
[3] CENA/^{14}C Laboratory, University of São Paulo, São Paulo, Brazil
[4] National Space Research Institute (INPE), São José dos Campos, Brazil
[5] CENA/Stable Isotopes Laboratory, University of São Paulo, Piracicaba, São Paulo
[6] Physics Department, LAC-UFF AMS Laboratory-Fluminense Federal University, Rio de Janeiro, Brazil

Received 24 November 2016; Revised 21 April 2017; Accepted 24 April 2017

*Correspondence to: Marcelo Cancela Lisboa Cohen, Federal University of Pará, Rua Augusto Corrêa, 01 – Guamá, CEP 66075-110, Belém (PA), Brazil. E-mail: mcohen80@hotmail.com

ESPL
Earth Surface Processes and Landforms

ABSTRACT: Generally, palaeoenvironmental interpretations consider only allogenic processes, when autogenic factors may have a strong influence on proxies of stratigraphic sequences. For instance, the Holocene history of the vegetation along the southern littoral of the State of Bahia in north-eastern Brazil is characterized by mangrove dynamics controlled by allogenic processes. However, over smaller timescales (~700 years), autogenic processes may have controlled vegetation dynamics and hence observed pollen distribution. This work proposes tidal channel dynamics as one of the main cause for changes in pollen assemblage along the studied stratigraphic profiles during the last centuries, based on sedimentology, pollen and elemental analysis ($\delta^{13}C$, $\delta^{15}N$ and C/N) and radiocarbon dating of sedimentary organic matter from two cores sampled from an abandoned meander and a tidal flat at the mouth of the Jucuruçu River. One core was sampled from a mangrove formed during the past ~550 cal yr BP. Another core recorded sediments in a *várzea* forest (swamp seasonally and permanently inundated by freshwater) located ~2.7 km from the current shoreline, which displayed a maximum age of ~680 cal yr BP. Two facies associations were identified: tidal channel (A) and tidal flat/oxbow lake (B). This work proposes allogenic processes as the main driving forces controlling the wetlands dynamics at the studied site during the Holocene. However, our data also reveal that part of the changes in vegetation over the last ~700 years reflect tidal channels and tidal flats development, which represent autogenic processes. The change in timescale analysis from the Holocene to recent centuries may have weakened the influence of allogenic factors. However, this needs interpretation with reference to the spatial scale of the depositional environment as the larger the depositional system analyzed, the stronger the influence of autogenic processes on stratigraphic sequences over longer timescales. Copyright © 2017 John Wiley & Sons, Ltd.

KEYWORDS: C and N isotopes; climate; Holocene; palynology, relative sea level

1. Introduction

Some paleoecological studies may be underestimating the autogenic impacts in the proxies used along stratigraphic sequences. Stratigraphy is controlled by the interaction of many autogenic and allogenic processes in cyclic sedimentation (Wanless and Shepard, 1936). These processes are separable by their physical and temporal scales. Allogenic processes include changes in energy and materials within a sedimentary system induced by processes external to the sedimentary system caused, for example, by sea-level change, tectonism, and climatic change, while autogenic processes operate locally, such as those intrinsic to the depositional system, involving the redistribution of energy and materials within a sedimentary system, and are of limited occurrence in time (Cecil, 2013). They are related to the action of tides and storms, channel avulsion, delta switching, lateral migration of meandering fluvial point-bars and beach-barrier bars, etc. (Beebower, 1964). Autogenic and allogenic processes interact and produce cycles of variable characteristics. Thus, differentiation of local versus regional and short-term versus long-term variations of cycle characteristics is critical to establishing a reliable stratigraphic interpretation (Schwarzacher, 1993).

Palaeoenvironmental reconstructions during the late Quaternary along the Brazilian littoral have indicated allogenic processes (sea-level and climate changes) as the main factors controlling coastal geomorphology and the distribution of vegetation types over time (Ledru *et al.*, 1996; Behling and da Costa, 2000; Behling *et al.*, 2001; Vedel *et al.*, 2006; Smith *et al.*, 2011; Cohen *et al.*, 2012, 2014; França *et al.*, 2012, 2014; Pessenda *et al.*, 2012; Buso Junior *et al.*, 2013; Guimarães *et al.*, 2013). In fact, the driving forces behind geomorphological and vegetation changes during the

Holocene may be explained by allogenic process (Busch and Rollins, 1984), since long-term sedimentation is generally driven by allogenic processes, which produce more widespread impacts on the sedimentary record than autogenic processes (Walker, 1992).

The mouth of the Jucuruçu River, in the south-eastern littoral of the State of Bahia, is characterized by wetlands with many abandoned meander channels and tidal flats. The present work aims to propose a model to explain the evolution of these wetlands and to evaluate the influence of autogenic and allogenic factors on proxies of stratigraphic sequences. To approach this issue, we carried out an investigation based on sedimentology, pollen data, isotope and elemental analysis ($\delta^{13}C$, $\delta^{15}N$, C/N) of the sedimentary organic matter and radiocarbon dating of two sediment cores sampled from a tidal flat occupied by mangrove (assemblages of salt tolerant trees and shrubs, mainly represented by the genus *Rhizophora*, *Avicennia* and *Laguncularia*, that grow in the intertidal zones of the tropical and subtropical coastlines) and *várzea* (swamp seasonally and permanently inundated by freshwater vegetation, *sensu* Parolin *et al.*, 2005).

2. Study Area

The study sites are located at the mouth of the Jucuruçu River that flows over Barreiras Formation into the coastal plain of southern Bahia. The Jucuruçu River originates in the municipality of Felisburgo (State of Minas Gerais) and flows east for approximately 330 km until its mouth in the city of Prado (State of Bahia). The stretch of sampling sites is influenced by saline and dynamic tides and presents some tidal channels within the mangrove forest. A coastal plateau and plain represent the main geomorphological features in the study area. The coastal plateau is represented by the Barreiras Formation (Miocene) that presents an abrupt contact with the coastal plain through a line of active and inactive cliffs. The coastal plain comprises Quaternary sediments of marine and estuarine origin, including marine terraces, lagoon terraces (muddy terraces), wetlands (mangroves/tidal plains, bog) and beaches (Andrade and Dominguez, 2002). The study site has a tidal range of 2 m (Directorate of Hydrography and Navigation (DHN), 2014) and is located adjacent to the 'Parque Nacional do Descobrimento' (PND) near the coastal town of Prado, southern Bahia, Brazil (Figure 1). The region is characterized by a warm and humid tropical climate with annual precipitation and temperature averaging 1350 mm and 24.5°C, respectively (Martorano *et al.*, 2003). The PND is a natural reserve with the original vegetation of the humid evergreen tropical rainforest (Atlantic Forest), where the most representative plant families are Fabaceae, Annonaceae, Myrtaceae, Sapotaceae, Mimosaceae, Moraceae, Melastomataceae, Arecaceae, Bignoniaceae, Lauraceae, Malpighiaceae, Lecythidaceae, Anacardiaceae, Euphorbiaceae, and Apocynaceae (Lima *et al.*, 2002; Peixoto and Gentry, 1990).

3. Materials and Methods

3.1. Remote sensing

The mapping of vegetation units from the study area was based on freely available remote sensing data. Landsat optical images acquired on April 2013 were downloaded from the Brazilian Institute of Space Research-INPE data bases. These optical images have a level 1 terrain (L1 T) processing, been radiometrically and geometrically corrected and orthorectified. A three-color band composition (Red) (Green) (Blue) (543) image was created and processed using the software SPRING 4.3.3 in order to discriminate the geomorphological features of interest.

Further processing included the digitalization of individual images showing vegetation boundaries and posterior layer overlap using georeferenced points to develop a time-series data set. Image texture, object size and shape features allowed a clear delimitation of the dense mangrove areas, due to the contrast with the adjacent vegetation types. Sample synthetic color images (2015, CNES/ASTRIUM) available from Google Earth (Yu and Gong, 2011) were used as a reference to characterize vegetation classes. These images present higher resolution than the Landsat images used for the temporal spatial analysis. The topographic data were derived from SRTM-30 m digital elevation model, downloaded from the United States Geological Survey (USGS) seamless data distribution system (http://srtm.usgs.gov/data/obtainingdata.html). Image interpretation of elevation data was carried out using the software Global Mapper 12. Twenty sites were selected for field validation of the satellite images and for more detailed evaluation of changes in vegetation cover.

3.2. Fieldwork and sample processing

The fieldwork occurred during the dry season of September 2014. The sediment cores PR 12 (1.92 m depth, S 17° 20′ 41.97" / W 39° 14′ 27.87") and PR 13 (1.48 m depth, S 17° 20′ 58.13″/W 39° 12′ 58.49″) were taken from tidal flats occupied by mangrove and transition between *várzea* and mangrove vegetation, respectively, using a Russian Sampler. The sampler uses a mechanism that prevents sediment compaction, because the sampler is inserted into the sediment in a closed position down to the desired sampling interval of 50 cm and then twisted so that the sediment column is trapped in the chamber. Visual observations and photographic documentation were used to determine the main geo-botanical units. The geographical positions of cores were determined by a global positioning system (GPS) using the SAD69 as reference datum.

3.3. Facies description

Following the methods of Walker (1992), facies analysis was undertaken, including description of color (Munsell, 2009), lithology, texture and structure. The sedimentary facies were codified following Miall (1978). The studied stratigraphic profile was divided into facies associations, with sedimentary units used to define a particular sedimentary environment (Reading, 1996). The cores were X-rayed to identify the sedimentary structures. Bulk samples (0.5 g each) were selected at 5 cm intervals for grain size analysis at the Chemical Oceanography Laboratory of the Federal University of Pará (UFPA), using a laser particle-size analyzer (SHIMADZU SALD 2201). Hydrogen peroxide (H_2O_2) was used to eliminate organic matter, while residual sediments were disaggregated by ultrasound. Calculation of grain-size distribution follows Wentworth (1922), with separation of sand (2–0.0625 μm), silt (62.5–3.9 μm) and clay (< 3.9 μm) fractions. In this study, sediment particles were identified only above 0.12 μm. Macroscopic analysis of surface sediments was also carried out, recording size, sorting and rounding of sandy sediments.

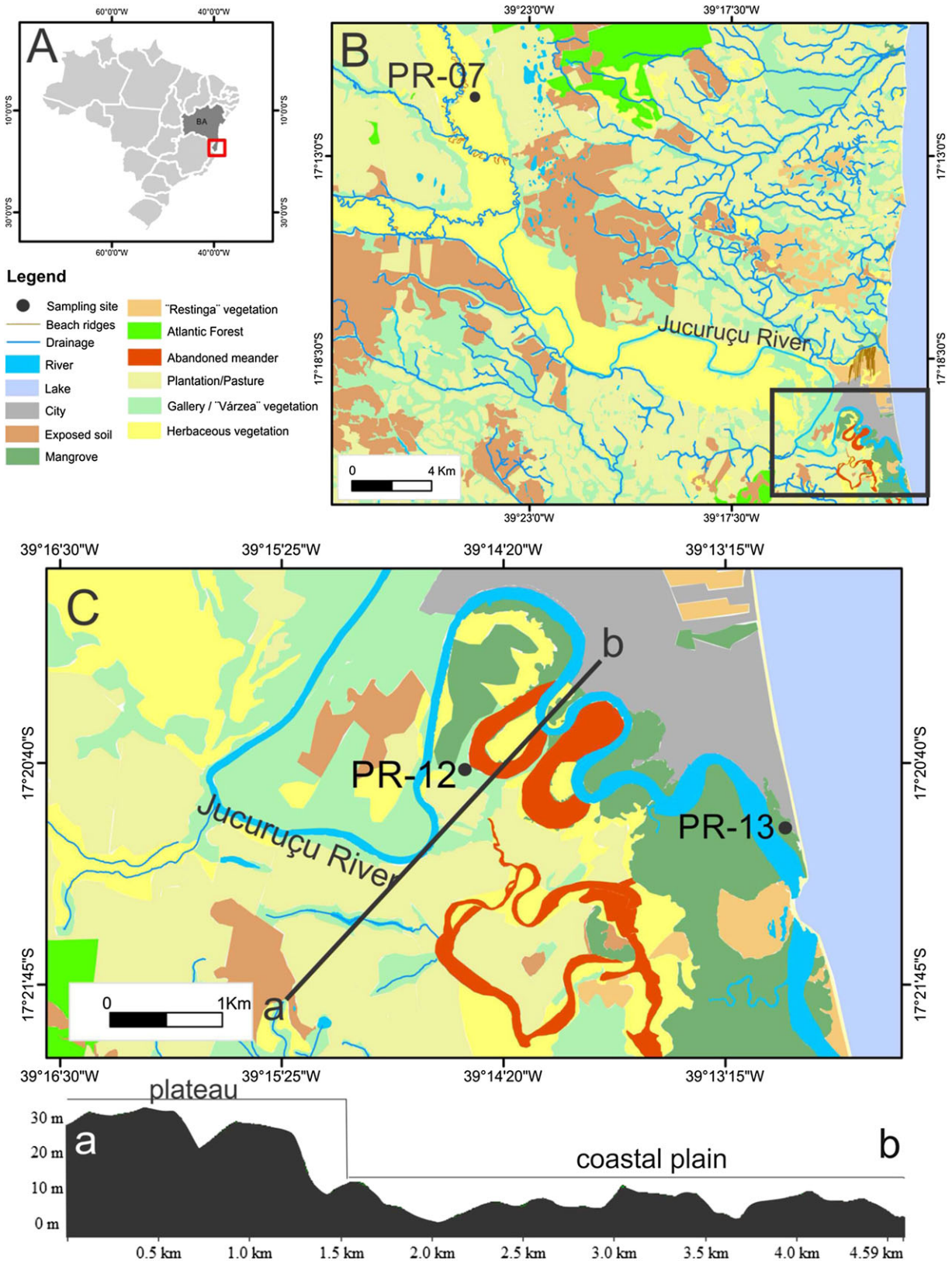

Figure 1. (A) Location of study area. (B) Vegetation map and geomorphological feature of study area. (C) Sampling sites of the studied cores and a topographic profile based on SRTM data. [Colour figure can be viewed at wileyonlinelibrary.com]

3.4. Pollen and spore analysis

Seventy 1-cm^3 samples were taken at 5 cm intervals through the cores for pollen analysis. All samples were prepared using standard pollen analytical techniques, including acetolysis (Erdtman, 1960). Sample residues were mounted on slides in a glycerin gelatin medium. Pollen and spores were identified by comparison with reference collections of about 4000 Brazilian forest taxa and various pollen keys (Salgado-Labouriau, 1973; Absy, 1975; Markgraf and D'Antoni, 1978; Roubik and Moreno, 1991; Colinvaux *et al.*, 1999), based on the reference collection of the Laboratory of Coastal Dynamics, UFPA, and the ^{14}C Laboratory of the Center for Nuclear Energy in Agriculture (CENA/USP).

An issue worth highlighting is the composition of a fossil pollen flora in sediments that depends on several factors:

1 Composition of the vegetation from which the pollen originates. The spatial representation of the lacustrine and tidal flats pollen signal depends on wind strengths and the extent of the drainage system feeding the lake and tidal flats. The proportion of the pollen signal provided by each vegetation type is distance-weighted (Davis, 2000; Cohen *et al.*, 2008; Xu *et al.*, 2012), with closer sources usually being greater.
2 Pollen production and dispersion of the individual plant species. Results on modern pollen accumulation rates from Bragança Peninsula, northern Brazil, indicate that among the mangrove taxa *Rhizophora* is a high pollen producer, while *Avicennia* and *Laguncularia* are low pollen producers (Behling *et al.*, 2001). This is plausible, because *Rhizophora* is wind pollinated, whereas *Avicennia* and *Laguncularia* are insect pollinated (Tomlinsom, 1986).
3 Pollen preservation in sediments may be influenced by various external factors (sediment grain size, microbial attack and oxidation), as well as factors inherent to the pollen grains themselves (sporopollenine content, chemical and physical composition of the pollen wall) (Havinga, 1967). Conversely, fine-grained sediment with high salinity and low Eh and pH values of mangroves are an appropriate environment for pollen preservation (Tschudy, 1969; Bryant *et al.*, 1994; Campbell and Campbell, 1994; Grindrod, 1988; Ellison, 2008; Phuphumirat *et al.*, 2015). Pollen tends to rapidly decay in sandy sediment because a better drainage in sand caused by large interstitial pores allows pollen grains to be abraded by a mobile inorganic matrix as well as to be oxidized during soil hydration–dehydration cycles (Faegri, 1971; Grindrod, 1988).

Then, changes in the pollen numbers in a sediment core may not necessarily reflect changes in vegetation or environmental conditions through time, but rather the poor fossilization potential of these pollen species. In this case, considering the changes in relationship between sand/mud sediments along the studied stratigraphic profiles, they possibly affect pollen concentrations, and these factors may cause misinterpretations regarding vegetation dynamics based on pollen concentration, thus the results of pollen analysis are shown as percentages.

The interval 100–150 cm of the core PR13 presented four samples with pollen concentrations lower than 10 000 g/cm^3, and three samples with absolute absence of pollen grains (Figure 2). The relatively low pollen concentration along the sandy layers was probably caused by large interstitial pores that allows pollen grains to be abraded and oxidized. Then, between 200 and 300 terrestrial pollen grains were counted for each sample. The levels with low pollen concentrations were considered in CONISS analysis, but the sediment layers with absolute absence of pollen grains have been removed and they are not considered by the cluster analysis. Pollen data were presented in pollen diagrams as percentages of the total pollen sum. The total pollen sum excludes fern spores, fungal spores, algae and micro-foraminifers. The taxa were grouped according to source: mangroves, trees and shrubs, palms, herbs and ferns. The software TILIA and TILIAGRAF were used for calculation and to plot the pollen diagram (Grimm, 1987). CONISS was used for cluster analysis of pollen taxa, permitting the zonation of the pollen diagram. CONISS is a program for stratigraphically constrained cluster analysis by incremental sum of squares. It has been used widely for unconstrained analyses and has proved particularly satisfactory for pollen frequency data (Grimm, 1987).

3.5. Isotopic and elemental analysis

A total of 70 samples (50–60 mg) were collected at 5 cm-intervals along the studied sediment cores. Sediments were treated with 4% hydrochloric acid (HCl) to eliminate carbonate, washed with distilled water until the pH reached 6, dried at 50°C, and finally homogenized. The samples were analyzed for total organic carbon (TOC) and total nitrogen (TN) at the Stable Isotope Laboratory of the CENA/USP. The results were expressed as a percentage of dry weight, with analytical precision of 0.09% (TOC) and 0.07% (TN), respectively.

The determinate of organic matter source will be environmental-dependent with $\delta^{13}C$, $\delta^{15}N$ and C/N composition (Lamb *et al.*, 2006), as follows: the C_3 terrestrial plants shows $\delta^{13}C$ values between −32‰ and −21‰ and

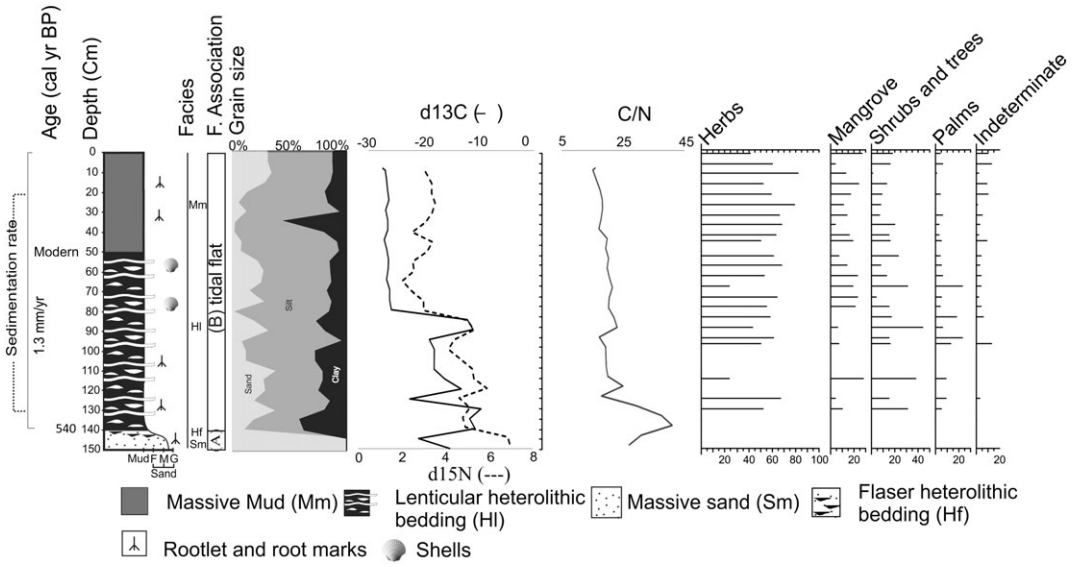

Figure 2. Summarized results for the core PR13, with variation as a function of core depth showing chronological and lithological profiles with sedimentary facies, as well as ecological pollen groups and geochemical variables. Pollen data are presented in the pollen diagrams as percentages of the total pollen sum.

C/N ratio > 12, while C_4 plants have $\delta^{13}C$ values ranging from −17‰ to −9‰ and C/N ratio > 20 (Deines, 1980; Meyers, 1997). Freshwater algae have $\delta^{13}C$ values between −25‰ and −30‰ (Meyers, 1997) and marine algae around −24‰ to −16‰ (Meyers, 1997). Meyers (1997) and Thornton and McManus (1994) used $\delta^{15}N$ values to differentiate organic matter from aquatic (> 10.0‰) and terrestrial plants (~0‰).

3.6. Radiocarbon dating

Based on color, lithology and/or texture discontinuities, five bulk samples (10 g each) were selected for radiocarbon analysis. In order to avoid natural contamination by shell fragments, roots, seeds, etc. (e.g. Goh, 1978), the sediment samples were physically cleaned under the stereomicroscope. Organic matter was extracted from the sediments according to the laboratory standard pre-treatment with acid–alkali–acid wash (Pessenda *et al.*, 2012). This procedure was used to remove fulvic and/or humic acids, which are potential sources of young carbon contaminants to the samples. This treatment consisted of extracting residual material with 2% HCl at 60°C during 4 h, followed by a rinse with distilled water to neutralize the pH. The samples were dried at 50°C. A detailed description of the chemical treatment for sediment samples can be found in Pessenda *et al.* (2012).

A chronologic framework for the sedimentary sequence was provided using accelerator mass spectrometry (AMS) dating at LACUFF (Fluminense Federal University, Niterói, Brazil) and at UGAMS (University of Georgia – Center for Applied Isotope Studies, Athens, GA). Radiocarbon ages were normalized to a $\delta^{13}C$ value of −25‰ VPDB and reported as calibrated years (cal yr BP) (2σ) using CALIB 6.0 and the SHCal13 curve (Reimer *et al.*, 2009). The dates are reported in the text as the median of the range of calibrated ages (Table I). The sedimentation rates were based on linear interpolation between age control points.

Table I. Sediment samples selected for radiocarbon dating with laboratory number, code site/depth, ^{14}C yr BP and calibrated (cal) ages

Laboratory (UGAMS)	*Sample/depth (cm)*	*^{14}C age years, BP*	*Calibrated (cal yr BP)*
21204	*PR13/70 cm*	*modern*	*modern*
21206	*PR13/140 cm*	*540 ± 20*	*519–557 (540)*
21207	*PR12/35 cm*	*modern*	*modern*
21208	*PR12/84 cm*	*350 ± 20*	*316–399 (350)*
21209	*PR12/173 cm*	*730 ± 25*	*655–701 (680)*

4. Results

4.1. Geomorphology and vegetation

The study site is located in a tidal flat near the mouth of the Jucuruçu River (Figure 1), which has a roughly linear northwest–southeast (NW–SE) orientation, flowing over crystalline rocks and the Barreira Formation into the coastal plain. This river changes upstream from low to high sinuosity, with abandoned meander channels and slightly sinuous straight channels downstream (Allen, 1970). Some lateral migration may be recorded with erosion of the outer channel margins and sedimentation in its inner margins. The fluvial deposits are predominantly comprised of moderately sorted, medium- to very coarse-grained sands, which extend from mountainous areas and Neogene tablelands. Muddy silt sediments characterize the tidal flats.

Examining Figure 1B, the plateaus are covered with a mixture of Atlantic Forest (10%), plantation/pasture (42%) and bare ground (11%), while the floodplains are dominated by herbaceous vegetation (13%). Gallery vegetation occurs along the scarps, mainly represented by Arecaceae, which covers 17% do the studied area. Downstream, muddy sediments spread over the floodplain and tidal flat that are occupied by *várzea* (freshwater vegetation) and mangrove (brackish water vegetation), respectively. Mangroves, which cover 8% of the studied area and close to the marine influence, occur as a fringe along tidal channels in the study area. They are characterized by *Rhizophora*, *Laguncularia* and *Avicennia.* Some tidal plains with mangroves are under erosive process. Coastal sand barriers, which parallel the shore, are colonized by *restinga* vegetation (*Ipomoea pes-caprae*, *Hancornia speciosa*, *Chrysobalanus icaco*, *Hirtella americana*, *Cereus fernambucensis* and *Anacardium occidentale*) and it covers about 16% of the studied area.

4.2. Radiocarbon date and sedimentation rates

The radiocarbon dates are shown in Table I. Considering the five radiocarbon ages along 3.4 m of sediment cores, two dates in the PR13 and three dates in the PR12 with a maximum interval of 1 m between each dating, no age inversions were observed (Figures 3 and 4). The samples PR13/70 cm and PR12/35 cm presented modern ages. Calculated sedimentary rates are 1.3 mm/yr (140–70 cm, PR13, Figure 3), 2.8 mm/yr (173–84 cm, PR12, Figure 4) and 2 mm/yr (84–0 cm, PR12). These rates are of the same order of magnitude as the vertical accretion interval of 0.1 and 11 mm/yr from mangrove forests

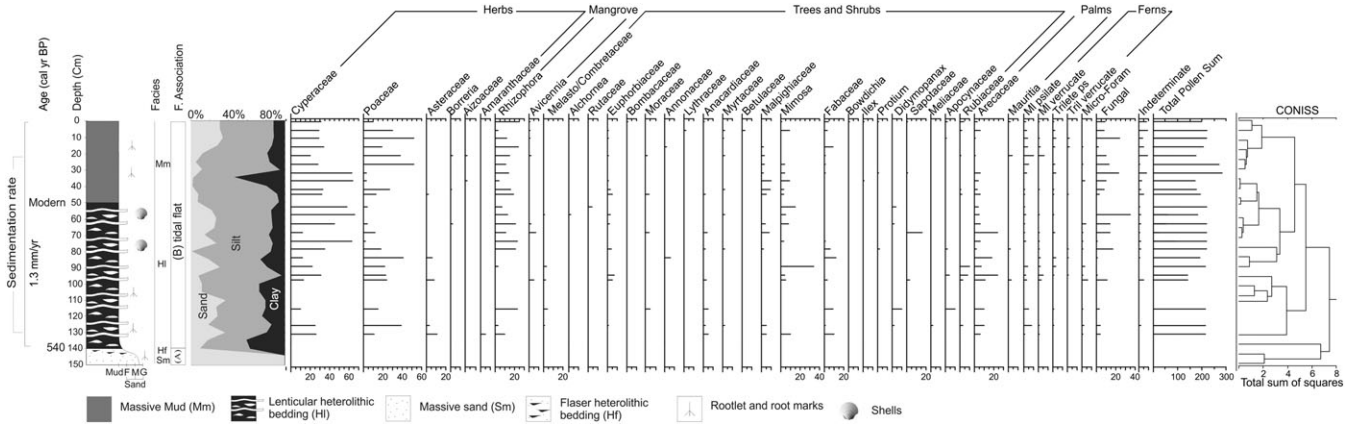

Figure 3. Pollen diagram of the core PR13, with percentages of the most frequent pollen taxa, samples age and cluster analysis.

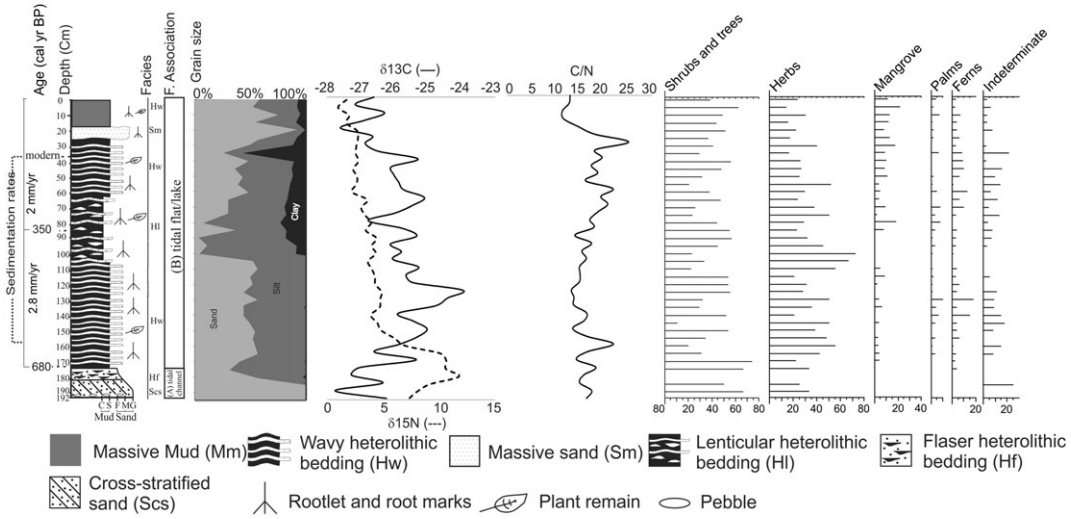

Figure 4. Summarized results for the core PR12, with variation as a function of core depth showing chronological and lithological profiles with sedimentary facies, as well as ecological pollen groups and geochemical variables. Pollen data are presented in the pollen diagrams as percentages of the total pollen sum.

reported by other authors (Cahoon and Lynch, 1997; Behling *et al.*, 2004; Vedel *et al.*, 2006; Cohen *et al.*, 2005a, 2005b, 2009; Guimarães *et al.*, 2010).

4.3. Facies and pollen description

The studied profiles consist mostly of grayish brown, grayish black or olive gray muds. Silt is the predominant grain size along the cores, but olive gray sand may be also present. In addition, the cores show lenticular, wavy or flaser heterolithic bedding and massive sands and muds (Figures 3 and 4). Bioturbation characterized by benthic organisms, mollusk shells, plant remains, roots and root marks are locally present. The integration of sedimentary facies, pollen data and geochemical records allowed to define two facies associations: (A) channel and (B) tidal flat/lake (Table II, Figures 2 and 4).

4.3.1. Facies association a (tidal channel)

Facies association A occurs at the base of the studied cores (> 550 cal yr BP, PR13, and >680 cal yr BP, PR12) (Figures 2 and 4). It consists of medium- to fine-grained sands arranged into a fining-upward cycle with quartz and plagioclase angular pebbles with a particle size of 5 to 40 mm on the basis (facies Sm), cross-stratified sand (Scs) and flaser heterolithic bedded deposits (Hf). Pollen grains along this facies association were found only in the core PR12 (192–175 cm depth, six samples) (Figure 5). This association contains pollen of trees and shrubs (50–67%) including Malpighiaceae (0–42%), Aquifoliaceae (0–33%), *Illex* (0–33%), Euphorbiaceae (0–17%), Rubiaceae (0–17%) and Anacardiaceae (0–17%). Mangrove and palm pollen are absent, and there is a dominance of pollen of herbs, mainly represented by Poaceae (45–55%), followed by Cyperaceae (40–50%), Amaranthaceae (3–5%), Astereceae and *Borreria* (~3%).

The $\delta^{13}C$ values in association A varied from approximately −27‰ to approximately −15‰ (mean −22‰) and the $\delta^{15}N$ from 7 to 11‰ (mean 8‰). The TOC results are relatively low (0.1–0.3%) at the bottom of the core, similarly to the TN (~0.01%). The C/N results are between 15 and 31 (Figures 2 and 4, Table II).

4.3.2. Facies association B (tidal flat/oxbow lake)

Facies association B occurs in the upper parts of the studied cores, where it consists of lenticular (Hl) or wavy (Hw) heterolithic bedded deposits (Hl), massive mud (Mm), and a small proportion (5 cm) of massive sand (Sm). Deposition occurred since ~550 cal yr BP (PR13) and ~680 cal yr BP (PR12).

The pollen assemblage includes four ecological groups (Figures 3 and 5). In the PR13, herbs (23–82%) are represented mainly by Cyperaceae (10–66%), Poaceae (2–52%), Asteraceae (0–11%) and Borreria (0–2%). Pollen grains of trees and shrubs (2 and 44%) are mainly of Mimosa (0–34%), Sapotaceae (0–15%), Fabaceae (0–12%), Malpighiaceae (0–10%), Apocynaceae (0–10%), Didymopanax (0–10%), Rubiaceae (0–9%), Euphorbiaceae (0–8%), Melastomataceae/Combretaceae (0–5%), Anacardiaceae (0–5%) and Moraceae (0–5%). Mangrove (0–29%) is represented by *Rhizophora* (0–26%) and *Avicennia* (0–8%). Pollen of Arecaceae occur between 0 and 23%.

Table II. Summary of facies association with sedimentary characteristics, predominance of pollen groups and geochemical data

Facies association	Facies description	Pollen predominace	Geochemical data	Interpretation
A	Massive sand (facies Sm) with medium to coarse grain size, cross-stratified sand (Scs) and *Flaser* heterolithic bedding (Hf), olive gray color, with vegetal fragments presence. Wavy (Hw) and lenticular heterolithic bedding (Hw). Small interval (5 cm) with massive sand (Sm) and massive mud (Mm).	Trees, shrubs and herbs	$\delta^{13}C$ = −27 to −15‰ $\delta^{15}N$ = 7 to 11‰ TOC = 0.1 to 0.3% TN = 0.01% C/*N* = 15 to 31	Tidal channel
B	Bioturbation characterized by plant remain, rootlet and root marks.	Herbs, mangroves, trees and shrubs, and palms	$\delta^{13}C$ = −27.37 to −10.63‰ $\delta^{15}N$ = 0.97 to 10.68‰ TOC = 0.41 to 15.49% TN = 0.01 to 1.14% C/*N* = 11 to 41	Tidal plain/lake

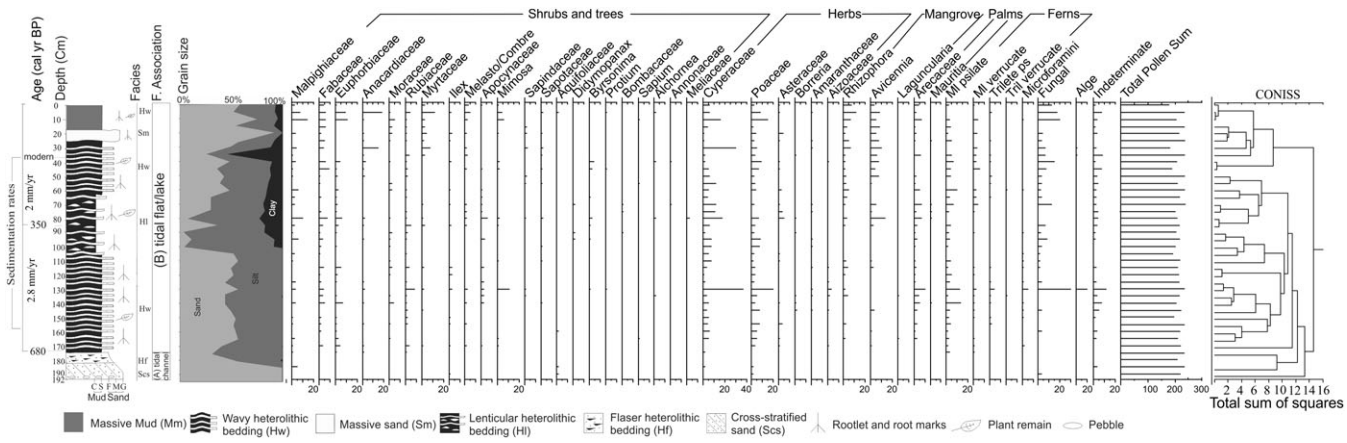

Figure 5. Pollen diagram of the core PR12, with percentages of the most frequent pollen taxa, samples age and cluster analysis.

Pollen assemblage in the core PR12 includes trees and shrubs (11–74%) mainly represented by Malpighiaceae (0–17%), Fabaceae (0–20%), Euphorbiaceae (0–17%), Anacardiaceae (0–16%), Moraceae (0–12%), Rubiaceae (0–15%), Myrtaceae (0–10%), *Illex* (0–23%), Melastomataceae/Combretaceae (0–8%), Apocynaceae (0–11%), Mimosa (0–9%), Sapindaceae (0–6%), *Byrsonima* (0–8%) and *Didymopanax* (0–6%). The herbs (14–73%) are characterized mostly by Cyperaceae (0–41%), Poaceae (0–32%), *Borreria* (0–7%) and Amaranthaceae (0–5%). The mangrove (0–40%) are represented mainly by *Rhizophora* (0–18%) and *Avicennia* (0–25%). Pollen of Arecaceae (0–16%) were also recorded along this facies association (Figure 5).

Facies association B in the core PR13 shows $\delta^{13}C$ and $\delta^{15}N$ values with an upward decreased trend from −10.63‰ to −27.37‰ (mean −22.3‰) ($r = 0.81$, $n = 27$, $p < 0.001$) and from 5.91‰ to 2.03‰ (mean 3.6‰) ($r = 0.71$, $n = 27$, $p < 0.001$), respectively. TOC and TN oscillated between 0.41% and 6.79% (mean 4.2%) and 0.01% to 0.47% (mean 0.2%), respectively. The C/N values revealed an upward decreased trend from 40 to 15 ($r = 0.70$, $n = 27$, $p < 0.001$) (Figure 2). In the core PR12, association B recorded an increased $\delta^{13}C$ trend from −26‰ to −24‰ from 175 to 125 cm depth ($r = 0.81$, $n = 12$, $p < 0.001$), and a decreased trend from −24‰ to −26‰ from 125 m depth to the surface ($r = 0.65$, $n = 25$, $p < 0.001$). The $\delta^{15}N$ values revealed an upward decreased trend from 11‰ to 1‰ (mean 3.8‰) ($r = 0.83$, $n = 36$, $p < 0.001$). The TOC and TN values oscillated between 2 and 15.5% (mean 6.7%) and 0.14 and 1.14% (mean 0.35%), respectively. The C/N values indicated an increased trend from 16 to 25 along the interval 175 to 30 cm depth ($r = 0.55$, $n = 29$, $p < 0.001$)., while from 30 to 0 cm depth there was a decreased trend from 25 to 13 ($r = 0.78$, $n = 7$, $p < 0.02$) (Figure 4).

5. Interpretation and Discussions

Considering the geomorphological characteristics of the study site (Figure 1C) and sedimentary features of the facies association A, it appears to be a product of channel filling by lateral accretion of a meander. Channel fills generally are characterized by sandy sediments arranged in fine upwards sequences with pebbles confined to the basal part with sharp and erosional surface (Thomas et al., 1987; Tucker, 2001). After the transition from a tidal channel to tidal flat at ~680 cal yr BP mangrove establishment occurred at the mouth of the Jucuruçu River. Core PR13 shows a dominance of C_4 terrestrial herbs in the lower part of the tidal flat facies association (~550 cal yr BP), followed by C_3 mangrove trees with some influence of species from the Atlantic forest that probably surrounded this wetland, which is suggested by the fact that taxa from this forest type are present today in the study area. The deposits in the core PR12 and geomorphological features (Figure 1C) indicate that after channel abandonment occurred an oxbow lake with fine-grained sediments at ~680 cal yr BP formed. During this time, mangroves were developing on tidal flats near this lake (Figure 6) with strong influence of trees and shrubs from the Atlantic forest in addition to herbs. The sedimentary organic matter was sourced from C_3 terrestrial plants and estuarine algae. The studied cores reveal that the establishment of mangrove vegetation was controlled by tidal channel dynamics. This interpretation is suggested considering the highly dynamic nature of the study site, as indicated by many abandoned channels, and erosion of the tidal flats colonized by mangroves.

Sediments corresponding to the phase of active channel deposition contain pollen and organic matter resulting from the reworking of channel margin deposits, therefore palaeovegetation interpretation based on pollen and organic matter deposited during active channel deposition must be seem with caution. However, lateral migration of a meander generally causes erosion of the outer channel margins and sedimentation in its inner margins. Lauer and Parker (2004) presented a morphodynamical model for a channel bed and bank top elevation evolution that specifically accounts for changes in channel depth over time. The model considers two grain sizes: one for sand, which interacts primarily with the bed, and one for mud, which interacts only with the floodplain. This model describes the evolution of the proportion sand and mud in the floodplain deposits. The greater the stability of floodplain, the greater the mud accumulation in relation to the sandy sediments

In the case of a meandering river system an oxbow lake may develop. This geomorphic feature is formed by cutoff and may remove more than a single meander in a given occurrence. The formation and infilling of oxbow lakes as the first phase of infill is strongly controlled by the diversion angle between the active channel and the abandoned channel. Oxbow lakes are eventually filled up with fine-grained overbank deposits and generally have a fining-upward trend (Ishii and Hori, 2016).

The stability of floodplains/tidal flats acquired by lateral migration of a meander or oxbow lake development favors mangrove expansion under brackish water influence. Pollen and sedimentary organic matter deposited during the tidal flat phase are valuable for reconstructing the palaeovegetation, because these materials are sourced from plants living during the sedimentation time (Figure 6). Therefore, mangroves

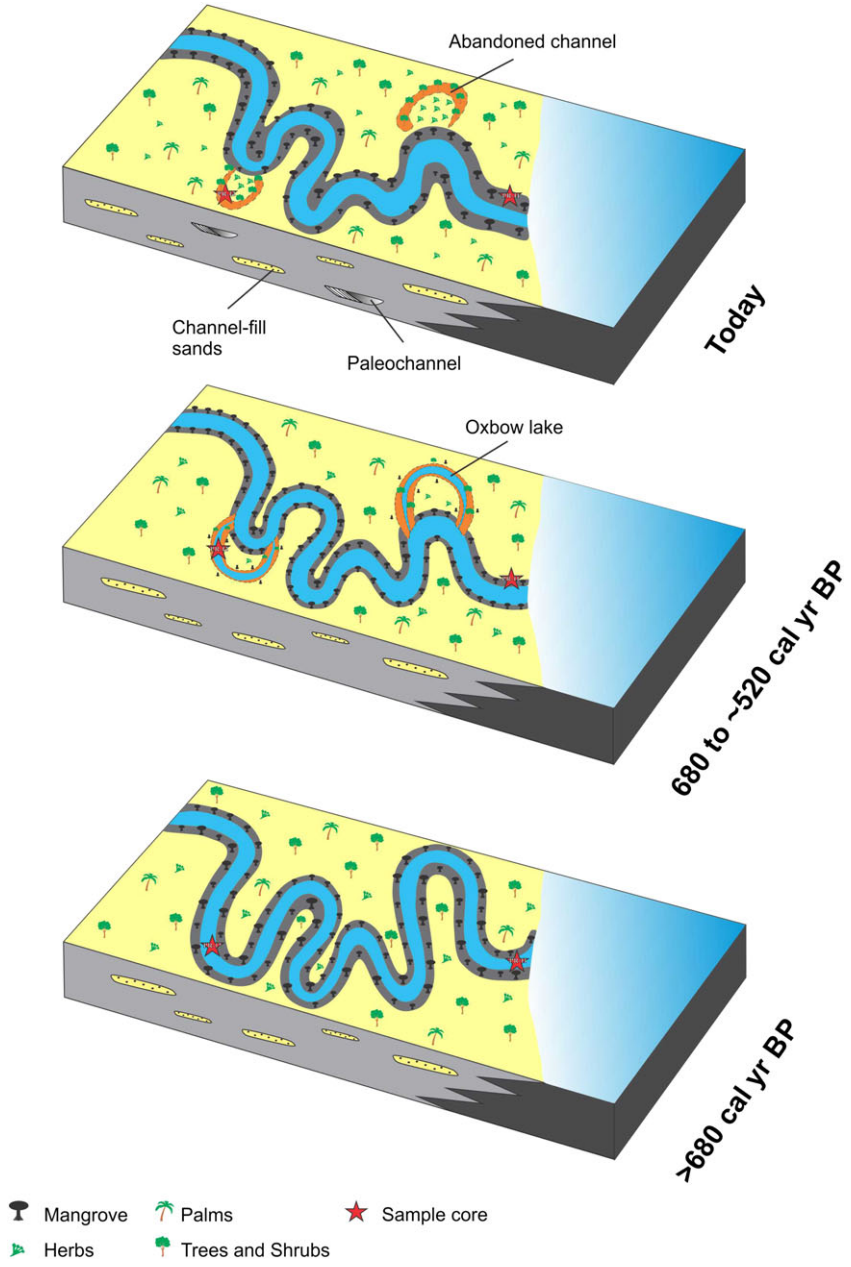

Figure 6. Model of channel dynamics influencing the mangrove establishment according to the phases: (1) active channel and (2) tidal plain/channel abandonment development. [Colour figure can be viewed at wileyonlinelibrary.com]

developed in tidal flats near the mouth of the Jucuruçu River since ~680 cal yr BP are probably a reflex of channel abandonment and tidal flat establishment.

The hypothesis of channel dynamics influencing the vegetation succession is in agreement with a study undertaken in the nearby Marajó Island (Rossetti *et al.*, 2010). These authors stated that a channel is fully abandoned and filled with sediment, its surface is occupied first by grasslands and then by terra firma forest.

Not all changes in coastal vegetation may be attributed to autogenic processes. For instance, a previous publication (Fontes et al., 2017) based on a multi-proxy analysis of one core (core PR07) located 23 km from the mouth of the Jucuruçu River (Figure 1B) revealed that the landscape was an estuarine system with tidal flats colonized by mangroves between ~7450 and ~5500 cal yr BP. During the past ~5500 cal yr BP, the mangroves shrank and herbaceous terrestrial vegetation expanded. Considering core PR07 was sampled from a floodplain with herbaceous vegetation positioned about 4.5 ± 1 m above the relative sea-level (RSL), this environmental change may signify a progressive rise in RSL, with the consequent marine incursion into the Jucuruçu River valley during the early to middle Holocene. Conversely, during the late Holocene, RSL fell, causing marine regression and the restriction of mangroves to the tidal flats near the modern coastline (Fontes et al., 2017).

The late Holocene was characterized by the disappearance of mangroves upriver and their seaward advance over the modern coast, where cores PR12 and PR13 were sampled (Figure 1C). Mangrove trees are currently positioned ~34 km away from the core PR07 previously acquired at the mouth of the Jucuruçu River. Considering its geomorphologic and topographic position, the environmental and vegetation changes identified along the core PR07 were attributed to allogenic processes (Fontes et al., 2017). This core presents a gradual increase in mangrove pollen along almost 3 m of tidal flat deposits accumulated during 2000 years interval (7500–5500 cal yr BP). During the last 5500 cal yr BP, the mangrove tidal flat changed into a fluvial plain occupied by herbs, and the isotope and elemental data indicate a change from estuarine

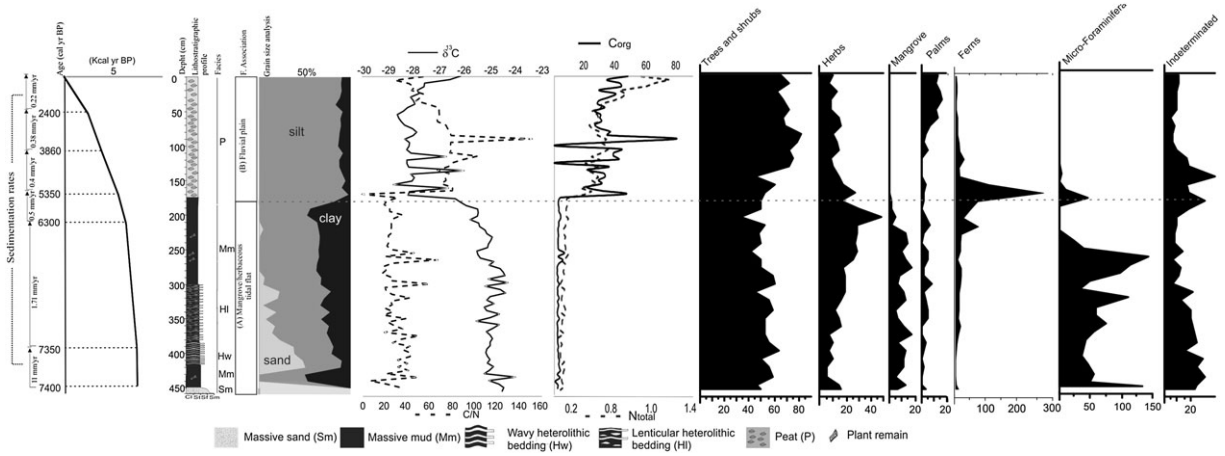

Figure 7. Summarized results for the core PR07, with variation as a function of core depth showing chronological and lithological profiles with sedimentary facies, as well as ecological pollen groups and geochemical variables. Pollen data are presented in the pollen diagrams as percentages of the total pollen sum (Fontes *et al.*, 2017).

organic matter to freshwater organic matter (Figure 7). The sedimentary environment during the past 7500 cal yr BP changed from a tidal flat into a fluvial floodplain characterized by changes in vegetation and in the source of organic matter. Noteworthy is the fact that during this time-frame, the sedimentary features (grains size and structures) did not indicate an active channel acting in reworking of channel margin deposits. Obviously, allogenic processes may cause changes in depositional environments and consequently in sedimentary features. However, in the case of PR07, its stratigraphic set associated with topographic and geomorphological data suggests that allogenic processes were the main driving forces leading to the changes in vegetation and source of organic matter in the study site during the Holocene.

Another example of allogenic processes controlling the palaeoflora is an integrated study focused on sedimentology, palynology**,** C and N isotopes, geochemical (Al, Ba, Ca, Cr, Fe, Mg, Mn, Na, Nb, P, Si, Sr and Ti) and radiocarbon dating of a sediment core from an herbaceous plain not flooded by tides from Amapá littoral, near the Amazon River mouth. It recorded a transition from marine to terrestrial influences at ~400 cal yr BP (Cohen et al., 2015). According to these authors, mangroves occurred over tidal mud flats between >5610–5470 and 470–310 cal yr BP. The absence of mangrove vegetation since 470–310 cal yr BP was followed by the transition of brackish water organic matter to terrestrial C_3 plants. In addition, the geochemical data indicate a decrease in seawater influence during this last time frame (Cohen et al., 2015). In this case, the sampling site in Amapá does not indicate an elongated and sinuous morphology above high-water level suggestive of channel abandonment. The geomorphological map suggests that the sampling site positioned on a topographically elevated surface not influenced by modern tides was instead a wide tidal flat. The replacement of mangroves by freshwater vegetation on topographically higher flats and its expansion to lower terrains were most likely caused by a RSL fall. This event was also associated with drier conditions, with lower rainfall during the second part of the last millennium. Thus, allogenic processes caused the vegetation changes during the last 500 cal yr BP in the Amapá littoral (Cohen et al., 2015).

It is probable that change of timescale of analysis from 7000 years to 700 years has weakened the influence of allogenic factors. However, this timescale should be correlated with the dimensions of the depositional environment. For instance, Jucuruçu River presents ~100 m of width, while some rivers in northern Brazil, with their floodplains occupied by freshwater marshes, exhibit more than 1 km of width (e.g. Amazonas ~8 km, Solimões ~3 km, Tocantins ~1.5 km). Then, in these cases the influence of autogenic processes may be amplified for a timescale of some thousand years. Therefore, the larger the depositional system analyzed, the stronger the influence of autogenic processes on stratigraphic sequences during a longer timescale.

6. Conclusions

The integrated analysis of cores PR12 and PR13, sampled from the mouth of the Jucuruçu River, with previously published data from the core PR07 sampled 23 km upstream of this river, indicate that allogenic processes were the main driving forces behind mangrove dynamics during the Holocene. However, the stratigraphic successions formed in cores PR12 and PR13 over the last 600 years revealed that wetland dynamics and changes in source of sedimentary organic matter reflect coastal evolution inherent to sedimentation. Such processes may have also controlled the preservation of pollen assemblies along the sedimentary succession corresponding to active channel followed by channel abandonment and/or tidal flat development.

Changes in coastal vegetation during a short timescale, as recorded in the study area, are not necessarily related to allogenic processes (i.e. eustatic and climatic fluctuations). Autogenic processes, such as those inherent to sediment dynamics, may also have controlled the pollen assembly along the studied profiles. However, it should be noted that considering the balance between the influence of allogenic and autogenic processes, conclusions regarding timescale cannot be made without considering the influence of the spatial scale of the depositional system.

Therefore, studies focusing upon the reconstruction of palaeovegetation require analyses based on a wide range of information that must integrate the identification of modern vegetation and of geomorphologic units with stratigraphic data based on descriptions of sedimentary facies, pollen assembly, as well as isotope and elemental data, in order to distinguish allogenic from autogenic processes.

Acknowledgements—The authors would like to thank the members of the Laboratory of Coastal Dynamics (LADIC-UFPA), the Center for Nuclear Energy in Agriculture (CENA-USP), the Vale Nature Reserve (Linhares, Brazil) and the students from the Laboratory of Chemical-Oceanography (UFPA). This study was financed by Fundação de

Amparo à Pesquisa do Estado de São Paulo (FAPESP) (03615-5/2007 and 00995-7/11), Conselho Nacional de Desenvolvimento Científico e Tecnológico (CNPQ) (470210/2012-5 and 405060/2013-0) and by the National Institute on Science and Technology in Tropical Marine Environments – INCT-AmbTropic (CNPq Process 565054/2010-4).

References

Absy ML. 1975. Polen e esporos do Quaternário de Santos (Brasil). *Hoehnea* **5**: 1–26.

Allen JRL. 1970. *Physical Processes of Sedimentation: Earth Science Series*. Elsevier: New York.

Andrade ACS, Dominguez JML. 2002. Informações geológico-geomorfológicas Como subsídios à análise ambiental: O exemplo da planície costeira de caravelas – Bahia. *Boletim Paranaense de Geociências* **51**: 9–17.

Beebower JR. 1964. Cyclothems and cyclic depositional mechanism in alluvial plain sedimentation. Bull. Kans. Univ. Geol. *Survey* **169**: 35–42.

Behling H, da Costa ML. 2000. Holocene environmental changes from the Rio Curuá Record in the Caxiuanã Region, eastern Amazon Basin. *Quaternary Research* **53**: 369–377.

Behling H, Cohen MCL, Lara RJ. 2001. Studies on Holocene mangrove ecosystem dynamics of the Bragança Peninsula in north-eastern Pará, Brazil. *Bosque* **167**: 225–242.

Behling H, Cohen ML, Lara R. 2004. Late Holocene mangrove dynamics of Marajó Island in Amazonia, northern Brazil. *Vegetation History and Archaeobotany* **13**: 73–80.

Bryant VMJ, Holloway RG, Jones JG, Carlson DL. 1994. Pollen preservation in alkaline soils of the American Southwest. In *Sedimentation of Organic Particles*, Traverse A (ed). Cambridge University Press: Cambridge.

Busch RM, Rollins HB. 1984. Correlation of Carboniferous strata using a hierarchy of transgressive-regressive units. *Geology* **12**: 471.

Buso Junior AA et al. 2013. From an estuary to a freshwater lake: a paleo-estuary evolution in the context of Holocene sea-level fluctuations, southeastern Brazil. *Radiocarbon* **55**: 1735–1746.

Cahoon DR, Lynch JC. 1997. Vertical accretion and shallow subsidence in a mangrove forest of southwestern Florida, U.S.A. *Mangroves and Salt Marshes* **1**: 173–186.

Campbell ID, Campbell C. 1994. Pollen preservation: experimental wet-dry cycles in saline and desalinated sediments. *Palynology* **18**: 5–10.

Cecil CB. 2013. An overview and interpretation of autocyclic and allocyclic processes and the accumulation of strata during the Pennsylvanian-Permian transition in the central Appalachian Basin, USA. *International Journal of Coal Geology* **119**: 21–31.

Cohen MCL, Behling H, Lara RJ. 2005a. Amazonian mangrove dynamics during the last millennium: the relative sea-level and the Little Ice Age. *Review Of Palaeobotany and Palynology* **136**: 93–108.

Cohen MCL, Souza Filho PWM, Lara RJ, Behling H, Angulo RJ. 2005b. A model of Holocene mangrove development and relative sea-level changes on the Bragança Peninsula (northern Brazil). *Wetlands Ecology and Management* **13**: 433–443.

Cohen MCL, Lara RJ, Smith CB, Angélica RS, Dias BS, Pequeno T. 2008. Wetland dynamics of Marajó Island, northern Brazil, during the last 1000 years. *Catena* **76**: 70–77.

Cohen MCL, Behling H, Lara RJ, Smith CB, Matos HRS, Vedel V. 2009. Impact of sea-level and climatic changes on the Amazon coastal wetlands during the late Holocene. *Vegetation History and Archaeobotany* **18**: 425–439.

Cohen MCL, Pessenda LCR, Behling H, de Fátima RD, França MC, Guimarães JTF, Friaes Y, Smith CB. 2012. Holocene palaeoenvironmental history of the Amazonian mangrove belt. *Quaternary Science Reviews* **55**: 50–58.

Cohen MCL, França MC, Rossetti DF, Pessenda LCR, Giannini PCF, Lorente FL, Buso JA, Castro D, Macario K. 2014. Landscape evolution during the late Quaternary at the Doce River mouth, Espírito Santo State, southeastern Brazil. *Palaeogeography, Palaeoclimatology, Palaeoecology* **415**: 48–58.

Cohen MCL, Alves ICC, França MC, Pessenda LCR, Rossetti D de F. 2015. Relative sea-level and climatic changes in the Amazon littoral during the last 500 years. *Catena* **133**: 441–451.

Colinvaux P, De Oliveira PE, Patiño JEM. 1999. *Amazon Pollen Manual and Atlas*. Harwood Academic Publishers: Dordrecht.

Davis MB. 2000. Palynology after Y2K — understanding the source area of pollen in sediments. *Annual Review of the Earth and Planetary Science* **28**: 1–18.

Deines P. 1980. The isotopic composition of reduced organic carbon. In *Handbook of Environmental Isotope Geochemistry. The Terrestrial Environments*, Fritz P, Fontes JC (eds). Elsevier: Amsterdam; 329–406.

Directorate of Hydrography and Navigation (DHN). 2014. Tide table. Porto De Ilhéus - Malhado - BA.

Ellison JC. 2008. Long-term retrospection on mangrove development using sediment cores and pollen analysis: a review. *Aquatic Botany* **89**: 93–104.

Erdtman G. 1960. The acetolysis method: in a revised description. *Svensk Botanisk Tidskrift Lund* **54**: 561–564.

Faegri K. 1971. The preservation of sporopollenin membranes under natural conditions. In *Sporopollenin*, Brooks J, Grant PR, Muir M, Gijzel PV, Shaw G (eds). Academic Press: London; 256–270.

Fontes NA, Moraes CA, Cohen MCL, Alves ICC, França MC, Pessenda LCR, Francisquini MI, Bendassolli JA, Macario K, Mayle F. 2017. The impacts of the middle Holocene high sea-level stand and climatic changes on Mangroves of the Jucuruçu River, southern Bahia – northeastern Brazil. *Radiocarbon* **59**: 215–230.

França MC, Francisquini MI, Cohen MCL, Pessenda LCR, Rossetti DF, Guimarães JTF, Smith CB. 2012. The last mangroves of Marajó Island — Eastern Amazon: impact of climate and/or relative sea-level changes. *Review of Palaeobotany and Palynology* **187**: 50–65.

França MC, Francisquini MI, Cohen MCL, Pessenda LCR. 2014. Inter-proxy evidence for the development of the Amazonian mangroves during the Holocene. *Vegetation History and Archaeobotany* **23**: 527–542.

Goh KM. 1978. Removal of contaminants to improve the reliability of radiocarbon dates of peats. *Journal of Soil Science* **29**: 340–349.

Grimm EC. 1987. CONISS: a FORTRAN 77 program for stratigraphically constrained cluster analysis by the method of incremental sum of squares. *Computers and Geosciences* **13**: 13–35.

Grindrod J. 1988. The palynology of holocene mangrove and saltmarsh sediments, particularly in northern Australia. *Review of Palaeobotany and Palynology* **55**: 229–245.

Guimarães JTF, Cohen MCL, França MC, Lara RJ, Behling H. 2010. Model of wetland development of the Amapá coast during the late Holocene. *Anais da Academia Brasileira de Ciências* **82**: 451–465.

Guimarães JTF, Cohen MCL, Franca MC, Pessenda LCR, Behling H. 2013. Morphological and vegetation changes on tidal flats of the Amazon Coast during the last 5000 cal. yr BP. *The Holocene* **23**: 528–543.

Havinga AJ. 1967. Palynology and pollen preservation. *Review of Paleobotany and Palynology* **2**: 81–98.

Ishii Y, Hori K. 2016. Formation and infilling of oxbow lakes in the Ishikari lowland, northern Japan. *Quaternary International* **397**: 136–146.

Lamb AL, Wilson GP, Leng MJ. 2006. A review of coastal palaeoclimate and relative sea-level reconstructions using δ13C and C/N ratios in organic material. *Earth-Science Reviews* **75**: 29–57.

Lauer JW, Parker G. 2004. Modeling channel-floodplain co-evolution in sand-bed streams; 1–10 http://ascelibrary.org/doi/10.1061/40737%282004%29181 [14 February 2017].

Ledru M-P, Braga PIS, Soubiès F, Fournier M, Martin L, Suguio K, Turcq B. 1996. The last 50,000 years in the Neotropics (Southern Brazil): evolution of vegetation and climate. *Palaeogeography, Palaeoclimatology, Palaeoecology* **123**: 239–257.

Lima JAS, Chagas CS, Manzatto CV, Assis DS, Perez DV, Pereira NR, Cunha TJF, Tosto SG. 2002. Distribuição de espécies arbóreas em fragmentos de vegetação natural no município de Prado - extremo sul da Bahia. *Rio de Janeiro, EMBRAPA, Circular Técnica* **17**: 4.

Markgraf V, D'Antoni HL. 1978. *Pollen Flora of Argentina*. University of Arizona Press: Tucson, AZ.

Martorano LG, Coutinho SC, Assis DS. 2003. Aspectos climáticos da região do Prado – BA. Rio de Janeiro: Embrapa Solos, 6 p.

(Agroclima. Comunicado Técnico, 13) http://ainfo.cnptia.embrapa.br/digital/bitstream/CNPS/11566/1/comtec13_2003_prado.pdf

Meyers PA. 1997. Organic geochemical proxies of paleoceanographic, paleolimnologic, and paleoclimatic processes. *Organic Geochemistry* **27**: 213–250.

Miall AD. 1978. Facies types and vertical profile models in braided river deposits: a summary. In *Fluvial Sedimentology*, Miall AD (ed). Canadian Society of Petroleum Geologists: Calgary; 597–604.

Munsell AH. 2009. *Munsell Soil Color Charts*. New Windsor, NY: Munsell Color Laboratory.

Parolin P, Müller E, Wolfgang J. 2005. Water relations of Amazonian várzea trees. *International Journal of Ecology and Environmental Sciences* **31**: 361–364.

Peixoto AL, Gentry A. 1990. Diversidade e composição florística da mata de tabuleiros na Reserva Florestal de Linhares (Espírito Santo, Brasil). *Revista Brasileira de Botânica* **13**: 19–25.

Pessenda LCR, Vidotto E, De Oliveira PE, Buso AA, Cohen MCL, de Rossetti DF, Ricardi-Branco F, Bendassolli JA. 2012. Late Quaternary vegetation and coastal environmental changes at Ilha do Cardoso mangrove, southeastern Brazil. *Palaeogeography, Palaeoclimatology, Palaeoecology* **363**: 57–68.

Phuphumirat W, Zetter R, Hofmann C-C, Ferguson DK. 2015. Pollen degradation in mangrove sediments: a short-term experiment. *Review of Palaeobotany and Palynology* **221**: 106–116.

Reading HG. 1996. *Sedimentary Environments: Processes, Facies and Stratigraphy*, third edn. Oxford: Blackwell Science.

Reimer PJ et al. 2009. IntCal09 and Marine09 radiocarbon age calibration curves, 0-50,000 years CAL BP. *Radiocarbon* **51**: 1111–1150.

Rossetti DF, Almeida S, Amaral DD, Lima CM, Pessenda LCR. 2010. Coexistence of forest and savanna in an Amazonian area from a geological perspective. *J. Veg. Sci.* **21**: 120–132.

Roubik DW, Moreno JE. 1991. *Pollen and Spores of Barro Colorado Island*. St Louis, MO: Missouri Botanical Garden.

Salgado-Labouriau ML. 1973. *Contribuição à palinologia dos cerrados*. Academia Brasileira de Ciências: Rio de Janeiro.

Schwarzacher W. 1993. *Cyclostratigraphy and the Milankovitch theory: Developments in Sedimentology*. Elsevier: London.

Smith CB, Cohen MCL, Pessenda LCR, França MC, Guimarães JTF, Rossetti D de F, Lara RJ. 2011. Holocene coastal vegetation changes at the mouth of the Amazon River. *Review of Palaeobotany and Palynology* **168**: 21–30.

Thomas RG, Smith DG, Wood JM, Visser J, Calverley-Range EA, Koster EH. 1987. Inclined heterolithic stratification—terminology, description, interpretation and significance. *Sedimentary Geology* **53**: 123–179.

Thornton SF, McManus J. 1994. Application of organic carbon and nitrogen stable isotope and C/N ratios as source indicators of organic matter provenance in estuarine systems: evidence from the Tay Estuary, Scotland. *Estuarine, Coastal and Shelf Science* **38**: 219–233.

Tomlinsom PB. 1986. *The Botany of Mangroves*. Cambridge University Press: Cambridge.

Tschudy RH. 1969. Relationship of palynomorphs to sedimentation. In *Aspects Of Palynology*, Tschudy RH (ed.) http://agris.fao.org/agris-search/search.do?recordID=US201301158396 [3 October 2015].

Tucker ME. 2001. *Sedimentary Petrology: An Introduction to the Origin of Sedimentary Rocks*. Blackwell Science: Oxford.

Vedel V, Behling H, Cohen M, Lara R. 2006. Holocene mangrove dynamics and sea-level changes in northern Brazil, inferences from the Taperebal core in northeastern Pará State. *Vegetation History and Archaeobotany* **15**: 115–123.

Walker RG. 1992. Facies, facies models and modern stratigrahic concepts. In *Facies Models – Response to Sea Level Change*, Walker RG, James NP (eds). Geological Association of Canada: Ontario; 1–14.

Wanless HR, Shepard FP. 1936. Sea level and climatic changes related to late Paleozoic cycles. *Geological Society of America Bulletin* **47**: 1177–1206.

Wentworth CK. 1922. A scale of grade and class terms for clastic sediments. *Journal of Geology* **30**: 377–392.

Xu Q, Tian F, Bunting MJ, Li Y, Ding W, Cao X, He Z. 2012. Pollen source areas of lakes with inflowing rivers: modern pollen influx data from Lake Baiyangdian, China. *Quaternary Science Reviews* **37**: 81–91.

Yu L, Gong P. 2011. Google Earth as a virtual globe tool for Earth science applications at the global scale: progress and perspectives. *International Journal of Remote Sensing* **33**: 3966–3986.